

Coexistence of shocks and rarefaction fans: complex phase diagram of a simple hyperbolic particle system

Márton Balázs^a Attila László Nagy^b Bálint Tóth^c István Tóth^d

December 3, 2024

Abstract

This paper investigates the non-equilibrium hydrodynamic behavior of a totally asymmetric attractive interacting particle system of particles, antiparticles, and holes on \mathbb{Z} . We explicitly compute the Eulerian hydrodynamic flux, which turns out to be neither concave nor convex in some regions of the model parameters. We characterize the entropy solutions of the Riemann problem in this scenario, some of them consisting of mixtures of rarefaction fans and shock waves. Our analysis is partially computer aided.

Keywords. Hydrodynamic limit, asymmetric particle system, non-equilibrium behavior, non-convex flux, Riemann problem, shock, rarefaction fan.

Acknowledgement. M. B. and B. T. acknowledge support from the grants OTKA K100473 and OTKA K109684. B. T. also thanks support from the Leverhulme International Network Grant “Laplacians, Random Walks and Quantum Spin Systems”.

1 Introduction

We focus on a particular nearest neighbor interacting particle system over \mathbb{Z} with one conserved quantity. The model consists of particles, antiparticles and holes with the following types of moves:

- (1) **Exclusion.** (Anti)particles execute totally asymmetric exclusions to the (negative) positive direction, respectively.
- (2) **Annihilation.** An adjacent particle-antiparticle pair can annihilate each other producing two holes.
- (3) **Pair creation.** An antiparticle-particle pair can be created from two adjacent holes.

The evolution is a continuous time Markov jump process the jump rates of which are chosen such that the model is *attractive* and possesses *product-form stationary distributions*. These choices greatly facilitate the analysis of the macroscopic behavior of the system. By rescaling time and space with the same factor (Eulerian scaling), we arrive to a hydrodynamic limit described by a nonlinear partial differential equation. As usual in this area nonlinearity comes from the *hydrodynamic flux* function.

In many well-known examples of particle systems, such as simple exclusion or constant rate zero range processes, this flux is strictly concave, sometimes strictly convex. Entropy solutions in these cases are well known: either shock wave or rarefaction fan emerges from step initial data, also called as Riemann problem. The novelty of the paper is that our simple model of just three possible states on a site has a flux with both concave and convex pieces as a function of the density. This gives rise to rather spectacular entropy solutions of the hydrodynamics from Riemann initial conditions. We characterize all possible cases for this model which can consist of coexisting shock wave and rarefaction fan regions in various orders depending on the density values we started off from. Parts of our investigations require the extensive use of the computer. Finally, we mention that most results of the present paper originate from [11]. Furthermore, [12] contains some nice simulation corresponding to the stochastic evolution rules of our model.

Organization of the paper. We define the microscopic model in Section 2. We calculate some of its key properties in Section 3. The detailed investigation of the Riemann problem is contained in Section 4.

^am.balazs@bristol.ac.uk, School of Mathematics, University of Bristol, UK.

^battilalaszlo.nagy@gmail.com, Institute of Mathematics, Budapest University of Technology and Economics, HU.

^cbalint.toth@bristol.ac.uk, School of Mathematics, University of Bristol, UK. MTA-BME Stochastics Research Group and Rényi Institute Budapest, HU.

^dtothi@math.bme.hu, Institute of Mathematics, Budapest University of Technology and Economics, HU.

2 The microscopic model

The Markov process we consider consists of particles, antiparticles and holes interacting with each other on the one-dimensional discrete torus $T_N := \mathbb{Z}/N\mathbb{Z}$ with periodic boundary conditions ($N \in \mathbb{N}$). At lattice point $i \in T_N$, ω_i will denote the presence of a particle ($\omega_i = 1$), that of an antiparticle ($\omega_i = -1$) or the absence of them ($\omega_i = 0$). Thus our configuration space is $\Omega_N := \{-1, 0, +1\}^{T_N}$ an element of which is denoted by $\boldsymbol{\omega} = (\omega_i)_{i \in T_N}$. The continuous time Markovian jump dynamics we attach on top of Ω_N is then made up of the moves

$$\boldsymbol{\omega} \longrightarrow \boldsymbol{\omega} - \delta_i + \delta_{i+1} \in \Omega_N,$$

which happens at rate $p(\omega_i, \omega_{i+1})$ for every $i \in T_N$, where δ denotes the Kronecker symbol, i.e. for each fixed $j \in \mathbb{Z}$: $(\delta_j)_i$ is 1 if $i = j$ and zero otherwise. These changes take place independently conditioned on a given configuration $\boldsymbol{\omega} \in \Omega_N$. Note that sites N and 0 are identified. This process can easily be constructed in the usual way (see [7]) and has infinitesimal generator \mathcal{G}_N acting on a periodic function $\varphi : T_N \rightarrow \mathbb{R}$ as

$$(\mathcal{G}_N \varphi)(\boldsymbol{\omega}) = \sum_{j=0}^{N-1} p(\omega_j, \omega_{j+1}) \cdot (\varphi(\boldsymbol{\omega} - \delta_j + \delta_{j+1}) - \varphi(\boldsymbol{\omega})) \quad (\boldsymbol{\omega} \in \Omega_N). \quad (2.1)$$

With a slight abuse of notation the state of the process at time $t \geq 0$ is also denoted by $\boldsymbol{\omega}(t) = (\omega_i(t))_{i \in \mathbb{Z}}$. We now specify p to be of the following special form. For $x, y \in \{-1, 0, +1\}$ let

$$p(x, y) = \begin{cases} c, & x = 0, y = 0; \\ a, & x = +1, y = -1; \\ a \cdot \frac{1-d}{2}, & x = 0, y = -1; \\ a \cdot \frac{1+d}{2}, & x = +1, y = 0; \\ 0, & \text{otherwise,} \end{cases} \quad (2.2)$$

where $a, c > 0$ are (distinct) model parameters denoting the rates of *annihilation* and *pair creation*, respectively. With parameter $d \in (-1, 1)$ we can adjust the symmetry of (anti)particles' jumping rate. In plain words, the above dynamics boils down to the following simple rules: two adjacent holes can produce an antiparticle-particle pair (in that order) with rate c , antiparticles and particles can only hop to the negative and positive directions with rates $a \cdot \frac{1-d}{2}$ and $a \cdot \frac{1+d}{2}$, respectively, and when a particle meets an antiparticle they annihilate each other with rate a . All other moves are suppressed.

By rescaling time by a , without loss of generality, we can assume that the annihilation rate is set to be 1. Next, we invoke the definition of *attractivity* from [7, pp. 72]. Formally speaking we require the relation $\mathbf{E} f(\boldsymbol{\omega}(t)) \leq \mathbf{E} f(\boldsymbol{\eta}(t))$ to hold for all monotone functions $f : \Omega_N \rightarrow \mathbb{R}$ and for all $t \geq 0$ whenever the initial configuration $\boldsymbol{\eta}(0)$ of $\boldsymbol{\eta}$ dominates that of $\boldsymbol{\omega}$ in the coordinate-wise order. In particular p is required to be monotone non-decreasing (non-increasing) in its first (second) variable, respectively. This means that our dynamics is attractive if and only if $c \leq \frac{1-|d|}{2}$ which we assume throughout the paper. We note that attractive processes are generally easier to handle.

The model outlined above is a member of the family of *misanthrope processes* [3], and first appeared in [10, pp. 180] in this particular form.

3 Properties of the model

In Subsection 3.1 we calculate the stationary distributions of the model, then Subsections 3.2 and 3.3 establish some of its hydrodynamic properties. These are then used in Section 4 to determine the entropy solution of the Riemann problem.

3.1 Stationary distribution

A very convenient feature of our model of rates (2.2) that it possesses *product-form stationary distributions*, this is shown next. First, we define

$$b := \frac{1}{2 + \frac{1}{\sqrt{c}}}, \quad (3.1)$$

which is a bijection between the parameters $c \in (0, \frac{1}{2}]$ and $b \in (0, \frac{1}{2+\sqrt{2}}]$. Now, let $\theta \in \mathbb{R}$ be a generic real that is also referred to as the *chemical potential*. Then define the one-site marginal measure by

$$\Gamma^\theta := (\Gamma^\theta(-1), \Gamma^\theta(0), \Gamma^\theta(1)) = \left(\frac{b \exp(-\theta)}{Z(\theta)}, \frac{1-2b}{Z(\theta)}, \frac{b \exp(\theta)}{Z(\theta)} \right), \quad (3.2)$$

with *partition sum* $Z(\theta) := 1 + 2b \cdot (\cosh(\theta) - 1)$. The product measure on Ω_N is built from these marginals: $\mathbf{\Gamma}^\theta := \bigotimes_{j \in T_N} \Gamma^\theta$. We denote the expectation with respect to this measure by \mathbf{E}^θ .

From general theory we know that $\mathbf{\Gamma}^\theta$ is *stationary* for the dynamics determined by (2.1) if and only if

$$\mathbf{E}^\theta[\mathcal{G}_N \varphi] = \sum_{\omega \in T_N} (\mathcal{G}_N \varphi)(\omega) \cdot \mathbf{\Gamma}^\theta(\omega) = 0$$

holds for every $\varphi : T_N \rightarrow \mathbb{R}$. To verify this identity we insert the definition of \mathcal{G}_N (2.1):

$$\mathbf{E}^\theta[\mathcal{G}_N \varphi] = \sum_{j=0}^{N-1} \sum_{\omega \in \Omega_N} p(\omega_j, \omega_{j+1}) \cdot \varphi(\omega_j - \delta_j + \delta_{j+1}) \cdot \mathbf{\Gamma}^\theta(\omega) - \sum_{j=0}^{N-1} \sum_{\omega \in \Omega_N} p(\omega_j, \omega_{j+1}) \cdot \varphi(\omega) \cdot \mathbf{\Gamma}^\theta(\omega),$$

then change a summation variable for each j in the first sum:

$$\sum_{\omega \in \Omega_N} p(\omega_j + 1, \omega_{j+1} - 1) \cdot \varphi(\omega_j) \cdot \frac{\Gamma^\theta(\omega_j + 1) \cdot \Gamma^\theta(\omega_{j+1} - 1)}{\Gamma^\theta(\omega_j) \cdot \Gamma^\theta(\omega_{j+1})} \cdot \mathbf{\Gamma}^\theta(\omega).$$

Here we took advantage of the product structure of $\mathbf{\Gamma}^\theta$ and the fact that Γ^θ is defined to be zero outside $\{-1, 0, 1\}$. Putting these together we obtain

$$\mathbf{E}^\theta[\mathcal{G}_N \varphi] = \sum_{j=0}^{N-1} \left(p(\omega_j + 1, \omega_{j+1} - 1) \cdot \frac{\Gamma^\theta(\omega_j + 1) \cdot \Gamma^\theta(\omega_{j+1} - 1)}{\Gamma^\theta(\omega_j) \cdot \Gamma^\theta(\omega_{j+1})} - p(\omega_j, \omega_{j+1}) \right) \cdot \varphi(\omega) \cdot \mathbf{\Gamma}^\theta(\omega).$$

Notice that the definition of measure Γ^θ (3.2) just implies

$$p(x + 1, y - 1) \cdot \frac{\Gamma^\theta(x + 1) \cdot \Gamma^\theta(y - 1)}{\Gamma^\theta(x) \cdot \Gamma^\theta(y)} = p(y, x)$$

whenever $x \in \{-1, 0\}$ and $y \in \{0, 1\}$ for our particular rates (2.2). Furthermore, notice that

$$\sum_{j=0}^{N-1} p(x_j, x_{j+1}) = \sum_{j=0}^{N-1} p(x_{j+1}, x_j),$$

which finishes the proof. Notice, however, that $\mathbf{\Gamma}^\theta$ is not *ergodic* since it does not respect the only invariant quantity of the system: the total (signed) particle number. Indeed, we obtain the extremal stationary measures by conditioning on this quantity.

Finally, we mention that our model is the simplest member, after simple exclusion, of the family detailed in [10, pp. 179] (see also [2]).

3.2 Hydrodynamics

Eulerian hydrodynamic limits are well established for a large class of asymmetric particle systems [8, 6, 5] or generally [1] that includes our model. Let N be the rescaling factor and define

$$u_N(x, t) := \mathbf{E}^{\theta_N} \omega_{\lfloor x/N \rfloor}(t/N)$$

as the rescaled density at macroscopic space and time $x \in \mathbb{R}$ and $t \geq 0$ ($\lfloor \cdot \rfloor$ denotes the integer part function). If the sequence of initial distributions is chosen properly then the limit

$$\lim_{N \rightarrow +\infty} u_N(x, t) = u(x, t)$$

exists for all continuity point x of $u(\cdot, t)$, and the *macroscopic density* $u : \mathbb{R} \times \mathbb{R}_0^+$ satisfies the conservation law

$$\begin{aligned} \partial_t u + \partial_x G(u) &= 0 \\ u(\cdot, 0) &= u_0(\cdot) \end{aligned} \tag{3.3}$$

with a Lipschitz continuous *hydrodynamic flux* G and initial condition $\lim_{N \rightarrow +\infty} u_N(x, 0) = u_0(x)$. In the following we will only consider the *Riemann problem*, i.e. the step initial condition

$$u_0(x) = \begin{cases} u_- & \text{if } x \leq 0; \\ u_+ & \text{if } x > 0, \end{cases} \tag{3.4}$$

where $u_- \neq u_+$ are the initial densities on the left as well as on the right-hand side of the origin.

We set these density values of u_0 by picking the appropriate site-dependent parameters θ_j of the product measure of marginals Γ^θ :

$$\mathbf{E}^{\theta_j}(\omega_j) = \begin{cases} u_- & \text{if } -[N/2] < j \leq 0; \\ u_+ & \text{if } 0 < j \leq [N/2]. \end{cases}$$

Indeed, it is more convenient to reparametrize Γ^θ with the (*signed*) *density* of particles instead of the chemical potential θ . Let $v(\theta)$ be the expected number of particles occupying an arbitrary lattice point under the measure Γ^θ :

$$v(\theta) := \mathbf{E}^\theta \omega_0 = \frac{2b \sinh(\theta)}{1 + 2b \cdot (\cosh(\theta) - 1)} \quad (\theta \in \mathbb{R}).$$

It is not hard to see that the assignment $\theta \mapsto v(\theta) \in [-1, 1]$ is strictly monotone hence bijective. Its inverse $v \mapsto \theta(v)$ can explicitly be calculated:

$$\theta(v) = \log \left(\frac{(1 - 2b) \cdot v + \sqrt{4b^2 + (1 - 4b) \cdot v^2}}{2b \cdot (1 - v)} \right) \quad (v \in [-1, 1]). \quad (3.5)$$

With a slight abuse of notation we will freely switch between these two parametrizations of the stationary measure.

To close this section, we mention a well-known strategy for solving (3.3). When G has continuous derivative and u is also smooth, one can rewrite (3.3) as $\partial_t u + G'(u) \cdot \partial_x u = 0$. The *characteristic curves* are then defined as lines of the x - t space along which the solution is constant. To find these curves one solves $\frac{d}{dt} u(x(t), t) = 0$, which translates to $\frac{dx(t)}{dt} = G'(u)$ after comparison to the original equation. The curve then can be traced back to the initial condition and takes the form $x = x_0 + t \cdot G'(u_0(x_0))$. The quantity $G'(u_0(x_0))$ is known as the *characteristic velocity*. Finally, to look up the value of the solution u at an arbitrary point $(x, t) \in \mathbb{R} \times \mathbb{R}_0^+$ one just follows the characteristic curve back to the initial time and reads the value of u_0 there.

This program relies on the assumption that u is smooth which sometimes just fails to happen. There can exist points of $\mathbb{R} \times \mathbb{R}^+$ which more than one characteristic lines hit carrying different initial values. In these cases classical (differentiable) solutions of (3.3) cease to exist and more general, so-called *weak solutions* need to be defined. By a careful selection of the weak solutions one can uniquely identify the physically relevant one which is also referred to as the *entropy solution*. For more details and properties of the entropy solutions we refer to the monographs [9, 4].

In our case, when the initial condition u_0 is the step function of (3.4) then the characteristic velocities can only attain two values: $G'(u_-)$ and $G'(u_+)$. Now, depending on the order of u_-, u_+ and on the monotonicity of G' in $[\min(u_-, u_+), \max(u_-, u_+)]$ several possibilities can emerge. In the simplest case when G is strictly concave we can essentially distinguish two cases: (1) if $G'(u_-) > G'(u_+)$ then the characteristic lines meet in some finite time hence a *shock wave*, that is a moving discontinuity appears in the entropy solution; (2) when $G'(u_-) < G'(u_+)$ then the characteristic lines are moving away from each other giving rise to a *rarefaction fan* in which the initial sharp discontinuity smears out in time.

In the general case, based on [4, pp. 30–34 of Section 2.2], the unique entropy solution of (3.3) with initial condition (3.4) can explicitly be given as

$$u(x, t) = \begin{cases} u_- & \text{if } x \leq (G_-)'(u_-) \cdot t; \\ [(G_-)']^{-1}(x/t) & \text{if } (G_-)'(u_-) \cdot t < x \leq (G_-)'(u_+) \cdot t; \\ u_+ & \text{if } x > (G_-)'(u_+) \cdot t, \end{cases} \quad (3.6)$$

where $u_- > u_+$ and G_- is the *upper concave envelope* of G defined to be the smallest concave function which is greater than or equal to G above the interval $[u_+, u_-]$. The derivative of G_- is denoted by $(G_-)'$, while its inverse by $[(G_-)']^{-1}$. Analogously, in the opposite case when $u_+ > u_-$ the solution can be obtained by the help of the *lower convex envelope* of G .

3.3 Flux

We now explicitly calculate the *hydrodynamic flux* G of (3.3) corresponding to our microscopic model. The flux is then defined to be the expected current rate across an arbitrary bond under the invariant measure Γ^θ , which was determined in Subsection 3.1, that is

$$G(v) = \mathbf{E}^{\theta(v)} p(\omega_0, \omega_1) = \sum_{x, y \in \{-1, 0, +1\}} p(x, y) \cdot \Gamma^{\theta(v)}(x) \cdot \Gamma^{\theta(v)}(y)$$

$$\begin{aligned}
&= \frac{1-d}{2} \cdot \Gamma^{\theta(v)}(0) \cdot \Gamma^{\theta(v)}(-1) + \frac{1+d}{2} \cdot \Gamma^{\theta(v)}(1) \cdot \Gamma^{\theta(v)}(0) \\
&\quad + c \cdot \Gamma^{\theta(v)}(0) \cdot \Gamma^{\theta(v)}(0) + 1 \cdot \Gamma^{\theta(v)}(1) \cdot \Gamma^{\theta(v)}(-1),
\end{aligned}$$

where $v \in [-1, 1]$. Notice that without explicit invariant measures the definition of G becomes quite subtle (see [1, Section 2.3]).

Now, substituting the measure $\Gamma^{\theta(v)}$ of (3.2) into the previous display we get

$$G(v) = \frac{b \cdot (1 - 2b) \cdot (\cosh(\theta(v)) + d \cdot \sinh(\theta(v))) + 2b^2}{(1 + 2b \cdot (\cosh(\theta(v)) - 1))^2}.$$

Note that G is *even* if and only if $d = 0$. Taking into consideration (3.5) we can realize the density parametrization of the flux. Elementary calculus then yields

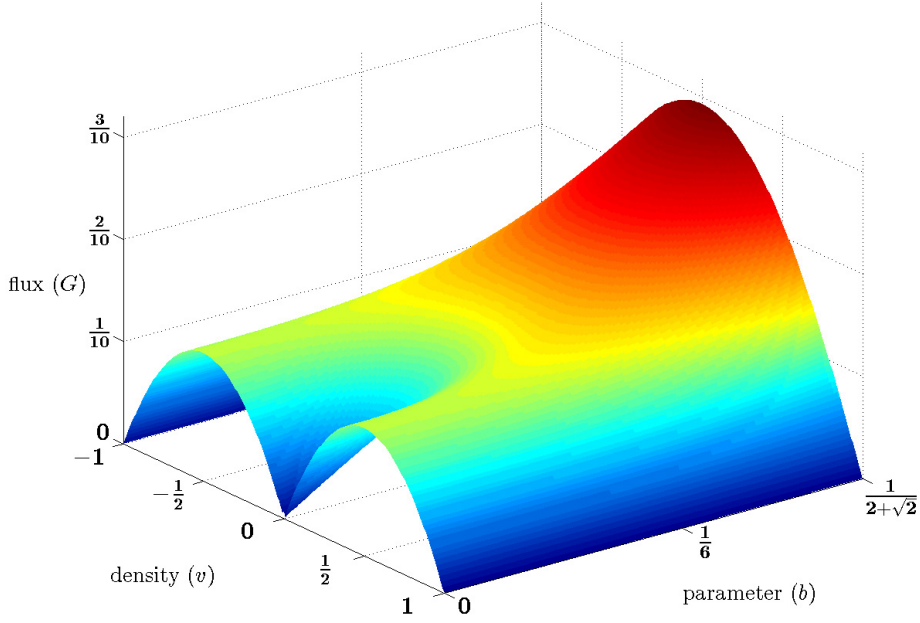


Figure 1. The hydrodynamic flux G , where a vertical slice of the surface gives a particular density-flux assignment for a b .

Theorem 1. *The hydrodynamic flux $G : [-1, 1] \rightarrow [0, +\infty)$ of our microscopic model (2.1) with rate (2.2) is given by*

$$G(v) = \frac{v \cdot (d - v)}{2} + \frac{(1 - d \cdot v) \cdot (4b^2 + (1 - 2b)^2 \cdot v^2)}{2(4b^2 + (1 - 2b) \cdot \sqrt{4b^2 + (1 - 4b) \cdot v^2})} \quad (v \in [-1, 1]),$$

where $b = \frac{1}{2+c^{-1/2}}$ and $c, d > 0$ (see (3.1)). In the symmetric case, i.e. $d = 0$, we obtain that

$$G(v) = -\frac{v^2}{2} + \frac{4b^2 + (1 - 2b)^2 \cdot v^2}{2(4b^2 + (1 - 2b) \cdot \sqrt{4b^2 + (1 - 4b) \cdot v^2})} \quad (v \in [-1, 1]). \quad (3.7)$$

In this latter case, when $b \in (\frac{1}{6}, \frac{1}{2+\sqrt{2}}] \iff c \in (\frac{1}{16}, \frac{1}{2}]$ ($b = \frac{1}{6} \iff c = \frac{1}{16}$), G is strictly (non-strictly) concave in $[-1, 1]$. Otherwise when $b \in (0, \frac{1}{6}) \iff c \in (0, \frac{1}{16})$ it is neither concave, nor convex having two inflection points

$$\pm v_{\text{infl}} = \pm \sqrt{\frac{(2b^2(1 - 2b))^2/3 - 4b^2}{1 - 4b}}, \quad (3.8)$$

which separate a concave-convex ($-v_{\text{infl}}$) and a convex-concave (v_{infl}) region, respectively.

Remark 1. The surface on Figure 1 shows (3.7) as a function of v and b . In the upcoming sections we will only investigate the symmetric case ($d = 0$).

4 Entropy solutions

In this section we find the entropy solutions of the Riemann problem (3.3) with step initial datum (3.4) for all possible pairs of initial densities $u_-, u_+ \in [-1, 1]$. Recalling Section 3.2, for purely concave flux two valid scenarios can only happen: the discontinuity at zero is preserved over time (*shock wave* forms) or it immediately smears out (*rarefaction fan* forms). As we have seen the flux G can be non-concave in some parameter regions and this results in plenty of qualitatively different solutions for (3.3) to be discussed in more details below.

Auxiliary calculations. Based on Theorem 1, we introduce some further notations being valid *only* in the range $b \in (0, \frac{1}{6})$. The positive global maximum point of (3.7) is given by

$$v_{\max} = \frac{1}{2} \sqrt{\frac{(1+2b)(1-6b)}{1-4b}},$$

while the negative one is at $-v_{\max}$. The maximum value is then $G(v_{\max}) = G(-v_{\max}) = (1-2b)^2/(8-32b)$. At 0 the tangent line is horizontal and G has a local minimum with $G(0) = b$. This tangent intersects the curve in two points symmetrically to the origin. The positive is at

$$v_0 = \sqrt{\frac{(1-2b)(1-6b)}{1-4b}},$$

while the negative one is at $-v_0$. See Figure 2.

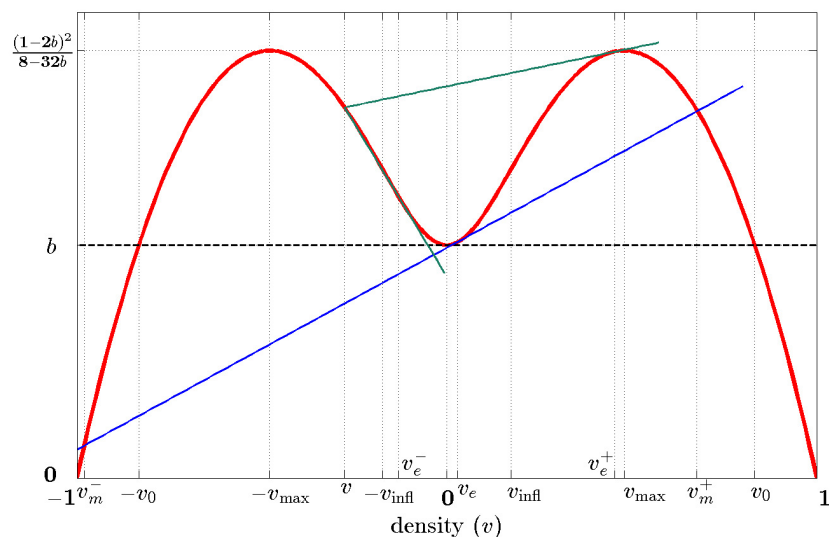


Figure 2. Hydrodynamic flux G in the non-concave case and its tangents

The tangent line drawn from the point $(v_e, G(v_e))$ intersects the graph G at (another) point $(v, G(v))$ if and only if it satisfies

$$G(v) = G(v_e) + G'(v_e)(v - v_e). \quad (4.1)$$

We can look at (4.1) in two different ways.

- One can look for an intersection $(v_m, G(v_m))$ of the graph and the tangent line touching at a *given* $(v_e, G(v_e))$. The intersection that lies on the left (right) of v_e is denoted by $v_m^-(v_e)$ [$v_m^+(v_e)$]. If $v_m^-(v_e)$ [$v_m^+(v_e)$] did not exist then $v_m^-(v_e) := -\infty$ [$v_m^+(v_e) := +\infty$]. See Figure 2.
- From a *fixed* $(v, G(v))$ one can solve (4.1) for a tangent point $(v_e, G(v_e))$ of G . If there exist more than one solutions then let $v_e^-(v)$ be the closer while let $v_e^+(v)$ be the farther one from v . By default $v_e(v) := v_e^-(v)$. If only one solution exists then $v_e(v) = v_e^-(v) = v_e^+(v)$. See Figure 2.

Phase diagram. Notice that if G'' does not change sign in $[\min(u_-, u_+), \max(u_-, u_+)]$, furthermore the secant of G connecting $(u_-, G(u_-))$ with $(u_+, G(u_+))$ is located *below* (*above*) its graph and

- $u_- < u_+$ ($u_- > u_+$), then the characteristic lines ‘converge’ and collide resulting in the formation of a *shock wave*.
- $u_- > u_+$ ($u_- < u_+$), then the characteristic lines ‘diverge’ and the initial discontinuity smoothens out according to the physically relevant entropy solution, i.e. a *rarefaction fan* forms.

Our first task is to explore these simple regions. Then in the general case we find the lower convex as well as upper concave envelopes of G which will give shock and rarefaction parts of the solution via formula (3.6). These functions can be expressed in a rather simple way by using the previously defined v_e 's and v_m 's.

The general case is as follows. Observe that if $b \geq \frac{1}{6}$ then shock wave (rarefaction fan) forms when $u_- < u_+$ ($u_- > u_+$). Henceforth we can assume that b belongs to $(0, \frac{1}{6})$. For the simpler parts of the phase diagram we can apply the above rule. Recall the inflection points of (3.8).

Shock wave (S) regions. If $u_- < u_+$, then $-1 \leq u_- \leq v_m^-(v_e(1))$ and $u_+ \geq v_m^+(v_e(u_-))$; $v_m^+(v_e(-1)) \leq u_+ \leq 1$ and $u_- \leq v_m^-(v_e(u_+))$; $-1 \leq u_- \leq -v_{\text{infl}}$ and $u_+ \leq v_e(u_-)$; $v_{\text{infl}} \leq u_+ \leq 1$ and $u_- \geq v_e(u_+)$. If $u_- > u_+$, then $u_-, u_+ \in [-v_{\text{infl}}, v_{\text{infl}}]$; furthermore $v_{\text{infl}} \leq u_- \leq v_{\text{max}}$ ($-v_{\text{max}} \leq u_+ \leq -v_{\text{infl}}$) and $v_e^+(u_-) \leq u_+ \leq v_m^-(u_-)$ ($v_m^+(u_+) \leq u_- \leq v_e^+(u_+)$).

Rarefaction fan (R) regions. If $u_- < u_+$, then $u_-, u_+ \in [-v_{\text{infl}}, v_{\text{infl}}]$. On the other hand, if $u_- > u_+$, then $u_-, u_+ \in [-1, -v_{\text{infl}}]$ or $u_-, u_+ \in [v_{\text{infl}}, 1]$.

Now, it becomes a much more complex situation if the secant crosses the graph of G above the interval $(\min(u_-, u_+), \max(u_-, u_+))$. We will discuss these in the following.

Rarefaction fan – Shock wave (RS) regions. If $u_- < u_+$, then $v_{\text{infl}} < u_+ \leq 1$ and $-v_{\text{infl}} \leq u_- < v_e(u_+)$. On the other hand if $u_- > u_+$, then $-v_{\text{max}} \leq u_+ < v_{\text{infl}}$ and $v_e^+(u_+) < u_- \leq 1$.

Shock wave – Rarefaction fan (SR) regions. If $u_- < u_+$, then $-1 \leq u_- < -v_{\text{infl}}$ and $v_e(u_-) < u_+ \leq v_{\text{infl}}$. On the other hand if $u_- > u_+$, then $-v_{\text{infl}} < u_- \leq v_{\text{max}}$ and $-1 \leq u_+ < v_e^+(u_-)$.

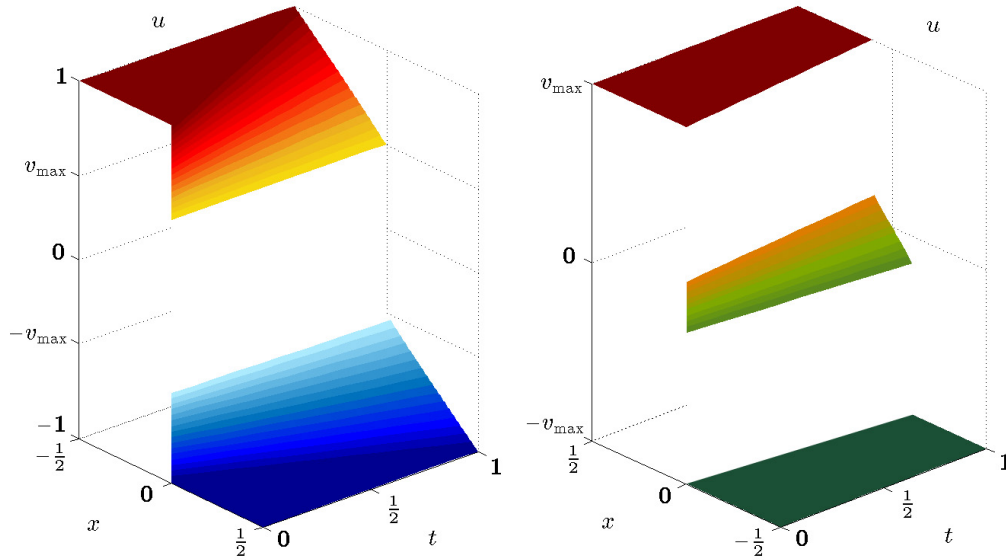


Figure 3. RSR (left) and SRS (right) when $u_- = 1 = -u_+$ and $u_- = -v_{\text{max}} = -u_+$, respectively.

Rarefaction fan – Shock wave – Rarefaction fan (RSR) region: $u_- > v_{\text{max}}$ and $u_+ < -v_{\text{max}}$. The shock wave in the middle has zero speed and $\lim_{x \rightarrow 0^+} u(x, t) - \lim_{x \rightarrow 0^-} u(x, t) = -2v_{\text{max}}$ for all $t > 0$. See Figure 3.

Shock wave – Rarefaction fan – Shock wave (SRS) region: $-1 \leq u_- < -v_{\text{infl}}$ and $v_{\text{infl}} < u_+ < v_m^+(v_e(u_-))$. The shocks are connected by a rarefaction fan and they are moving away from each other. See Figure 3.

The schematic picture of the whole phase diagram can be seen on Figure 4. The x and y axes correspond to the initial density on the left (u_-) and the right (u_+), respectively. ‘S’ denotes the formation of a shock wave, while ‘R’ corresponds to a rarefaction fan.

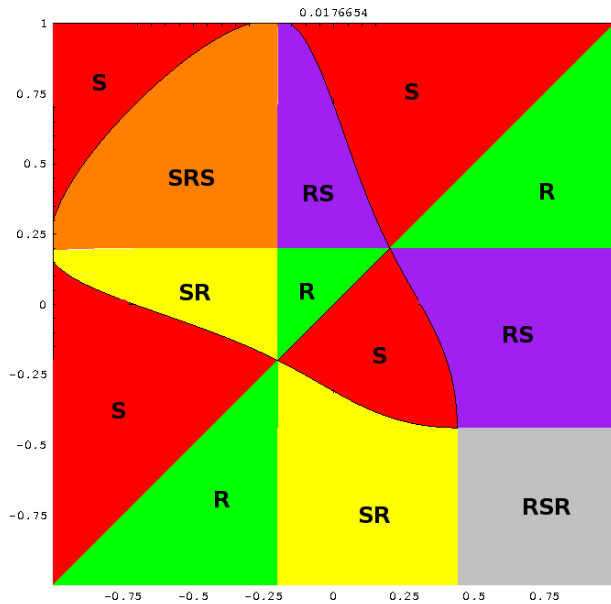


Figure 4. Phase diagram of the model when $b = \frac{21}{200}$ ($c \approx 0.01767$).

References

- [1] C. Bahadoran, H. Guiol, K. Ravishankar, and E. Saada. Euler hydrodynamics of one-dimensional attractive particle systems. *Ann. Probab.*, 34(4):1339–1369, 2006.
- [2] M. Balázs. Growth fluctuations in a class of deposition models. *Ann. Inst. H. Poincaré Probab. Statist.*, 39(4):639–685, 2003.
- [3] C. Coccozza-Thivent. Processus des misanthropes. *Z. Wahrsch. Verw. Gebiete*, 70(4):509–523, 1985.
- [4] H. Holden and N. H. Risebro. *Front Tracking for Hyperbolic Conservation Laws*. Springer, 2011.
- [5] C. Kipnis and C. Landim. *Scaling Limits of Interacting Particle Systems*. Springer, 1999.
- [6] C. Landim. Conservation of local equilibrium for attractive particle systems on \mathbb{Z}^d . *Ann. Probab.*, 21(4):1782–1808, 1993.
- [7] T. M. Liggett. *Interacting Particle Systems*. Springer, 1985.
- [8] F. Rezakhanlou. Hydrodynamic limit for attractive particle systems on \mathbb{Z}^d . *Comm. Math. Phys.*, 140(3):417–448, 1991.
- [9] J. Smoller. *Shock Waves and Reaction-Diffusion Equations*, Springer, 1983.
- [10] B. Tóth and B. Valkó. Between equilibrium fluctuations and Eulerian scaling: perturbation of equilibrium for a class of deposition models. *J. Stat. Phys.*, 109(1):177–205, 2002.
- [11] I. Tóth. Hydrodynamic behavior of an interacting particle system (in Hungarian). Master’s Thesis, Budapest University of Technology and Economics, Department of Stochastics, 2005.
- [12] I. Tóth. Simulation of a totally asymmetric attractive interacting particle system. Public link: <https://github.com/tothi/riemann-nonconvex/>, 2016.